Insights into Imaging

ESR EUROPEAN SOCIETY OF RADIOLOGY

ORIGINAL ARTICLE

Open Access

Check for updates

Inter-vendor and inter-observer reliability of diffusion tensor imaging in the musculoskeletal system: a multiscanner MR study

Vito Chianca[1,2]* , Domenico Albano[3], Stefania Rizzo[1], Mario Maas[4,5], Luca Maria Sconfienza[3,6] and Filippo Del Grande[1]

Abstract

Background To evaluate the inter-observer and inter-vendor reliability of diffusion tensor imaging parameters in the musculoskeletal system.

Methods This prospective study included six healthy volunteers three men (mean age: 42; range: 31–52 years) and three women (mean age: 36; range: 30–44 years).

Each subject was scanned using different 3 Tesla magnetic resonance scanners from three different vendors at three different sites bilaterally. First, the intra-class correlation coefficient was used to determine between-observers agreement for overall measurements and clinical sites. Next, between-group comparisons were made through the non-parametric Friedman's test. Finally, the Bland–Altman method was used to determine agreement among the three scanner measurements, comparing them two by two.

Results A total of 792 measurement were calculated. ICC reported high levels of agreement between the two observers. ICC related to MD, FA, and RD measurements ranged from 0.88 (95% CI 0.85–0.90) to 0.95 (95% CI 0.94–0.96), from 0.85 (95% CI 0.81–0.88) to 0.95 (95% CI 0.93–0.96), and from 0.89 (0.85–0.90) to 0.92 (0.90–0.94).

No statistically significant inter-vendor differences were observed. The Bland–Altmann method confirmed a high correlation between parameter values.

Conclusion An excellent inter-observer and inter-vendor reliability was found in our study.

Key points

1. Diffusion tensor imaging shows excellent inter-observer reliability.
2. Diffusion tensor imaging shows excellent inter-vendor reliability.
3. Quantitative results in musculoskeletal application of diffusion tensor imaging are reproducible in all the three magnetic resonance scanners.

*Correspondence:
Vito Chianca
vitochianca@gmail.com
Full list of author information is available at the end of the article

Chianca *et al. Insights into Imaging*   (2023) 14:32

Page 2 of 9

4. DTI, as a reproducible magnetic resonance sequence, can be used for a quantitative evaluation of muscle microstructures during daily practice.

Introduction

Since its first clinical application in the musculoskeletal (MSK) system, muscle diffusion tensor imaging (m-DTI) has become a valuable sequence for the evaluation of architectural changes of fibre microenvironments [1–4]. M-DTI provides parameters such as fractional anisotropy (FA), radial diffusivity (RD), and mean diffusivity (MD) that allow extracting quantitative information on integrity of muscle fibres [5, 6]. Inflammatory pathologies, traumatic injuries, neuromuscular disorders, or atrophic conditions are the principal areas of application of m-DTI in conjunction with conventional sequences in the assessments of early structural changes [7–11].

Furthermore, post-processing of DTI is able to generate fibre tractography and to assess 3D muscular structure from the origin to distal insertion by calculating architectural parameters such as fibre length, number and volume, and pennation angle [12].

Despite its potential to assess structural changes of the muscles, the application of m-DTI in clinical practice is still controversial because of several factors influencing DTI signals, such as field strength, gradient strength, b-values, and post-processing algorithms [13]. Several studies reported an acceptable agreement of DTI measurements on the brain, whereas m-DTI studies, which were mainly conducted on lower limb muscle group, reported relatively high variations with FA values ranging from 0.28 to 0.6 [6, 14]. Moreover, some studies on brain DTI reported conflicting results regarding inter-site, intra-site, and inter-vendor reliability [15–17]. To the best of our knowledge, no studies assess m-DTI inter-vendor agreement. The aims of our study were to assess the inter-reader reliability and the inter-vendor reliability on 3 T magnetic resonance (MR) for m-DTI measurements.

Materials and methods
Study subjects

The local ethics committee approved our prospective study, and all participants signed an informed consent before starting the examination. The study was conducted in compliance with the Declaration of Helsinki.

We enrolled six healthy volunteers: Three were males (mean age: 42; range: 31–52 years) and three women (mean age: 36; range: 30–44 years).

Inclusion criteria were: 18 year or older, no neuromuscular diseases in their personal and/or family history, no present or past muscle strains in the muscular group under evaluation, and no participation in any sports activity three weeks before the examination.

Exclusion criteria for enrolment were: usual contraindications to MR imaging, positive pregnancy test, and objects in the body that could obscure the target muscle groups through artefacts. After having optimized the sequences in collaboration with the specialists of the different vendors, each volunteer was scanned once on three different anatomical sites bilaterally (middle third of the arm, middle third of the leg, and middle third of the thigh). All scans were acquired on the same day within 6 h to reduce any possible bias and were checked for image quality and artefacts.

MR examination

MR examinations were performed using three 3 T (T) MR of our institution: Signa Pioneer (GE Healthcare, Milwaukee, WI, USA), Achieva (Philips Healthcare, Best, Netherlands), and Skyra (Siemens Healthineers, Erlangen, Germany). The total MR examination time for Signa Pioneer, Achieva, and Skyra was 18.05, 17.56, and 17.52 min, respectively. MR protocol acquisition parameters including RF-coils are summarized in Tables 1 and 2.

Image analysis

Following data acquisition and after removing all patient identifying information, a radiologist with eight years of experience in MSK MR interpretation assessed image quality [18]. Then, m-DTI parameters on different muscle compartments were independently assessed by two radiologists (8 and 10 years of experience in the MSK field) using a commercially available software (Olea sphere 3.0). The muscle regions of interest (ROIs) were selected as described in Fig. 1. Post-processing was performed on the DTI images. Motion-related misalignments and adjacent image noise were corrected with automated image registration. Both readers manually drew the ROIs on the same slices at the middle third of the thigh, leg, and arm on axial T1w sequences as shown in Fig. 1. FA, RD, and MD values of the different muscle areas were calculated. Fibre tractography of the thigh, leg, and arm is shown in Fig. 2.

Chianca *et al. Insights into Imaging* (2023) 14:32

Page 3 of 9

Table 1 DTI acquisition parameters

	GE	Philips	Siemens
DTI parameters (Thigh)			
Coil	16 channels	32 channels	18 channels
Directions	12	15	12
b-value (s/mm^2)	400	400	400
TR (ms)	7350	7500	7500
TE (ms)	Minimum	72	83.0
Matrix	128 × 128	128 × 128	128 × 128
Parallel factor	2 (asset)	2 (sense)	2 (grappa)
Voxel size (mm)	3.1 × 3.1 × 4.0	3.03 × 2.97 × 4.0	3.1 × 3.1 × 4.0
Acquisition time (minutes:seconds)	3.18	4.07	3.32
DTI parameters (leg)			
Coil	16 channels	32 channels	18 channels
Directions	12	12	12
b-value (s/mm^2)	400	400	400
TR (ms)	7950	7500	7500
TE (ms)	Minimum	66	83
Matrix	128 × 128	128 × 128	128 × 128
Parallel factor	2 (asset)	2 (sense)	2 (grappa)
Voxel size (mm)	2.3 × 2.3 × 4.0	2.3 × 2.3 × 4.0	2.3 × 2.3 × 4.0
Acquisition time (minutes:seconds)	3.35	4.07	3.32
DTI parameters (arm)			
Coil	16 channels	8 channels	18 channels
Directions	12	12	12
b-value (s/mm^2)	400.0	400	400
TR (ms)	8600	7837	7900
TE (ms)	Minimum	79	83
Matrix	122 × 122	122 × 122	122 × 122
Parallel factor	2 (asset)	2 (sense)	2 (grappa)
Voxel size (mm)	1.6 × 1.6 × 4.0	1.6 × 1.6 × 4.0	1.6 × 1.6 × 4.0
Acquisition time (minutes: seconds)	3.52	4.18	3.43

Statistical analysis

Results are reported as medians and interquartile ranges (IQR). Data distributions were checked for normality using the Shapiro–Wilk test, which showed that all data were non-normally distributed ($p < 0.05$). Next, the intra-class correlation coefficient (ICC) was used to determine between-observers agreement for overall measurements and clinical sites, keeping in this last case, the distinction between left and right side, so to use the contralateral side as a double check of agreement. Next, between-group comparisons were made through the nonparametric Friedman's test. We applied Friedman's test for each observer's measurements to prevent biased findings. Finally, the Bland–Altman method was used to determine agreement among the three scanner measurements, comparing them two by two. A p value less than 0.01 was considered to be statistically significant. Statistical analyses were executed by MedCalc Statistical Software version 19.2.6 (MedCalc Software bv, Ostend, Belgium; https://www.medcalc.org; 2020).

Results

Agreement between observers

The ICC reported high levels of agreement between the two observers as summarized in Table 3.

Good to excellent ICC values (higher than 0.69) were assessed between the two observers according to anatomical sites, except for FA measurement on Siemens MR (0.62, 95% CI 0.43–0.76). Detailed results are reported in Table 4.

Inter-vendor reliability

No statistically significant inter-vendor differences were observed for both readers and for all the parameters.

Chianca *et al. Insights into Imaging* (2023) 14:32

Page 4 of 9

Table 2 T1 TSE acquisition parameters

|	GE	Philips	Siemens
Thigh			
TR (ms)	604	519	600
TE (ms)	Minimum	13	11
Matrix	448	448	448
Parallel factor	2 (asset)	(2 sense)	2 (grappa)
Voxel size (mm)	0.9 × 0.9 × 4.0	0.9 × 0.9 × 4	0.9 × 0.9 × 4.0
Acquisition time (minutes: seconds)	2.01	1.36	1.52
Leg			
TR (ms)	618	519	600
TE (ms)	Minimum	13	11
Matrix	384 × 384	384 × 384	384 × 384
Parallel factor	2 (asset)	2 (sense)	2 (grappa)
Voxel size (mm)	0.8 × 0.8 × 4.0	0.8 × 0.8 × 4.0	0.8 × 0.8 × 4.0
Acquisition time (minutes: seconds)	1.49	1.33	1.38
Arm			
TR (ms)	635.0	519	605.0
TE (ms)	Minimum	13	11.0
Matrix	256 × 256	256 × 256	256 × 256
Parallel factor	2 (asset)	2 (sense)	2 (grappa)
Voxel size (mm)	0.7 × 0.7 × 4.0	0.7 × 0.7 × 4.0	0.7 × 0.7 × 4.0
Acquisition time (minutes: seconds)	1.40	1.25	1.29
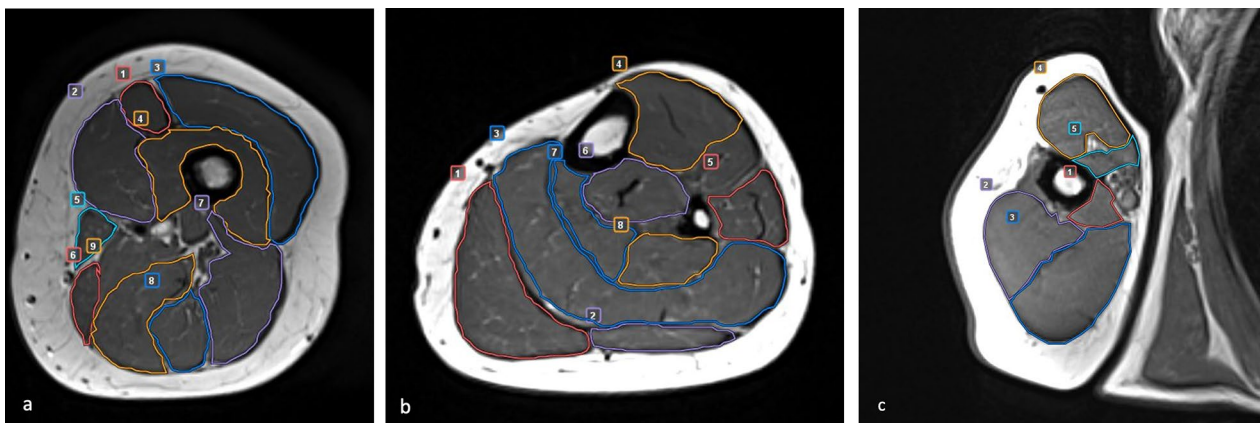
Fig. 1 Axial T1w images showing ROIs of the different anatomical compartments. **a** 1 rectus femoris, 2 vastus medialis, 3 vastus lateralis, 4 vastus intermedius, 5 sartorius, 6 gracilis, 7 biceps femoris, 8 semitendinosus, 9 semimembranosus. **b** 1 Medial gastrocnemius, 2 lateral gastrocnemius, 3 soleus, 4 anterior tibialis, 5 peroneal muscles, 6 posterior tibialis, 7 flexor digitorum longus, 8 flexor hallucis longus. **c** 1 Medial head of triceps brachii, 2 lateral head of triceps brachii, 3 long head of triceps brachii, 4 biceps brachii, and 5 coraco brachialis

(Table 5). MD measurements for reader two were close to significance ($p = 0.0573$).

Bland–Altman plots comparing MD (Fig. 3), FA (Fig. 4), and RD (Fig. 5), were drawn. The Bland–Altmann method confirmed a high correlation between parameter values due to the slight deviation obtained in the mean values and the difference between them: All values were drawn in the limits of agreement (LoA ± 1.96 standard deviation).

Discussion

Our study shows almost perfect inter-reader reliability for MD, FA, and RD on three different MR scanner and overall no statically significance differences among
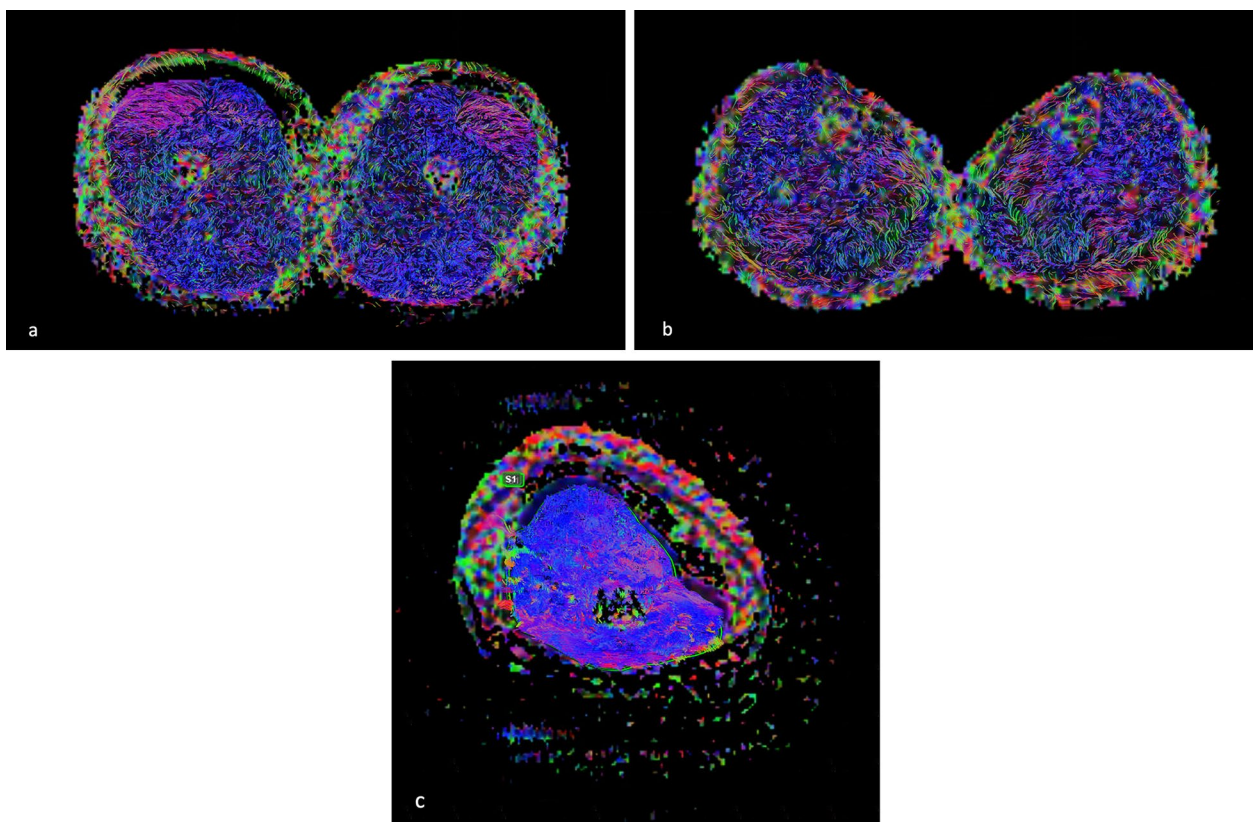
Fig. 2 Axial color FA map with overlaid tractography of the thighs (**a**), legs (**b**), and arm (**c**)

Table 3 Intra-class correlation

	GE	Philips	Siemens
MD	0.95 (0.94–0.96)	0.92 (0.90–0.94)	0.88 (0.85–0.90)
FA	0.91 (0.88–0.93)	0.95 (0.93–0.96)	0.85 (0.81–0.88)
RD	0.89 (0.86–0.91)	0.92 (0.90–0.94)	0.89 (0.85–0.90)

Table 4 ICC for clinical sites

	GE	Philips	Siemens
MD			
Right arm	0.97 (0.95–0.99)	0.89 (0.78–0.95)	0.76 (0.56–0.88)
Left arm	0.96 (0.91–0.98)	0.96 (0.93–0.98)	0.69 (0.44–0.84)
Right thigh	0.92 (0.87–0.95)	0.94 (0.90–0.96)	0.94 (0.89–0.96)
Left thigh	0.94 (0.89–0.96)	0.86 (0.77–0.91)	0.97 (0.94–0.98)
Right leg	0.94 (0.91–0.97)	0.96 (0.93–0.98)	0.91 (0.84–0.95)
Left leg	0.96 (0.94–0.98)	0.88 (0.79–0.93)	0.92 (0.86–0.95)
FA			
Right arm	0.96 (0.92–0.98)	0.86 (0.73–0.93)	0.88 (0.76–0.94)
Left arm	0.71 (0.49–0.85)	0.92 (0.83–0.96)	0.94 (0.87–0.97)
Right thigh	0.93 (0.88–0.96)	0.96 (0.93–0.98)	0.62 (0.43–0.76)
Left thigh	0.97 (0.94–0.98)	0.94 (0.90–0.96)	0.96 (0.94–0.98)
Right leg	0.86 (0.76–0.92)	0.93 (0.89–0.96)	0.93 (0.88–0.96)
Left leg	0.93 (0.88–0.96)	0.95 (0.92–0.97)	0.87 (0.77–0.92)
RD			
Right arm	0.98 (0.95–0.99)	0.89 (0.78–0.94)	0.84 (0.69–0.92)
Left arm	0.96 (0.93–0.98)	0.96 (0.92–0.98)	0.99 (0.98–0.99)
Right thigh	0.92 (0.86–0.95)	0.93 (0.89–0.96)	0.92 (0.87–0.95)
Left thigh	0.93 (0.89–0.96)	0.87 (0.79–0.92)	0.97 (094–0.98)
Right leg	0.95 (0.90–0.97)	0.94 (0.90–0.97)	0.90 (0.83–0.94)
Left leg	0.96 (0.93–0.98)	0.87 (0.78–0.93)	0.89 (0.81–0.94)

the three different vendors. A slightly decrease of inter-reader agreement was detected on Skyra MR for FA measurement in the right thigh. We suppose that this is due to the inclusion of tiny fatty areas of the subcutaneous tissue within the ROI [19].

Similar to previous studies on the nervous system, in our study the DTI values showed slightly statistical differences among different muscles as reported in Additional file (1) [13, 15, 18–20]. We assessed highest FA (0.348; IQR: 0.097) on gracilis muscle and lowest FA on vastus intermedius (second observer GE FA = 0.229; IQR: 0.038). Nevertheless, we believe that these differences, albeit slightly statically different, are not clinically significant because there is no overlapping between our FA values and those reported in patients

Chianca *et al. Insights into Imaging* (2023) 14:32

Page 6 of 9

Table 5 Inter-vendor differences in MD, FA, and RD

	GE Median (IQR)	Philips Median (IQR)	Siemens Median (IQR)	*p* value*
1° Observer				
MD	1.563 (0.295)	1.533 (0.253)	1.571 (0.346)	0.1152
FA	0.303 (0.059)	0.299 (0.071)	0.300 (0.072)	0.3772
RD	1.319 (0.257)	1.301 (0.252)	1.340 (0.318)	0.1643
CV of MD	0.17	0.14	0.23	–
CV of FA	0.15	0.16	0.17	–
CV of RD	0.18	0.15	0.23	–
2° Observer				
MD	1.559 (0.299)	1.541 (0.264)	1.592 (0.356)	0.0573
FA	0.301 (0.059)	0.300 (0.069)	0.300 (0.067)	0.7046
RD	1.320 (0.283)	1.312 (0.258)	1.343 (0.344)	0.3258
CV of MD	0.18	0.14	0.23	–
CV of FA	0.15	0.16	0.19	–
CV of RD	0.18	0.14	0.25	–

*p value was determined through Friedman's Test

MD mean diffusivity, *RA* radial anisotropy, *FA* fractional anisotropy, *RD* radial diffusivity, *CV* coefficient of variation

with spinal muscular atrophy or muscular dystrophies ranging from 0.7 to 0.41 [9, 23–25]. Our results support the findings found by Fourè and colleagues who reported some differences among the FA values of the muscles of the lower limb [26]. However, values of the different muscles reported in this study are slightly different compared to ours. We believe that value discrepancies between the two studies may be due to different magnetic fields strength that determines higher SNR provided by acquisition on 7 T which improve fibre tracking compared to 3 T [27, 28].

Another study conducted on ten volunteers showed good reproducibility on both 3 and 7 T MR (Siemens Healthcare GmbH, Erlangen, Germany) with an SNR increase in the 7 T MR of up to 111% [12]. However, on the 7 T MR, the authors found higher FA and lower MD values in the soleus muscle, while the results of the remaining muscle compartments did not show significant statistical difference of the quantitative values between the MR. The authors justified the heterogeneity
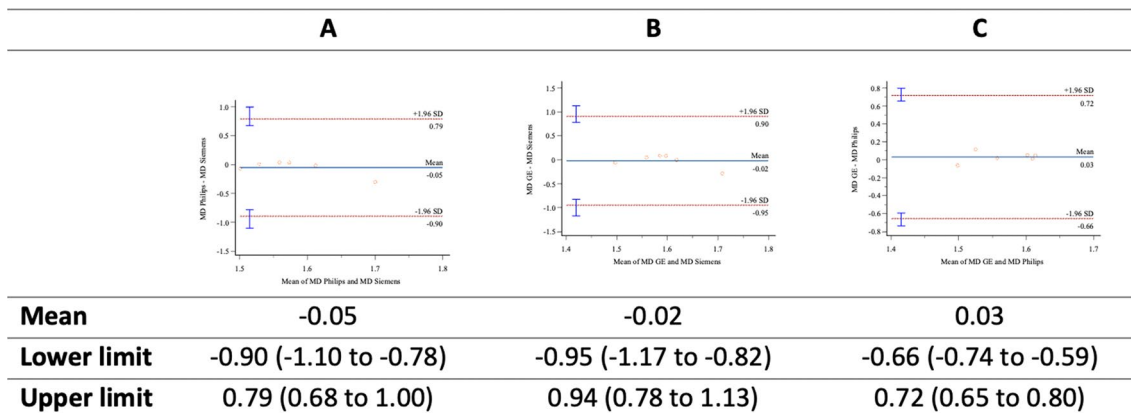

	A	B	C
Mean	-0.05	-0.02	0.03
Lower limit	-0.90 (-1.10 to -0.78)	-0.95 (-1.17 to -0.82)	-0.66 (-0.74 to -0.59)
Upper limit	0.79 (0.68 to 1.00)	0.94 (0.78 to 1.13)	0.72 (0.65 to 0.80)

Fig. 3 MD-**A**: Philips versus Siemens; **B**: GE versus Siemens; **C**: GE versus Philips

	A	B	C
Mean	-0.001409	-0.001977	-0.0005682
Lower limit	-0.1397 (-0.1506 to -0.1305)	-0.1381 (-0.1490 to -0.1289)	-0.1228 (-0.1330 to -0.1144)
Upper limit	0.1368 (0.1277 to 0.1478)	0.1341 (0.1250 to 0.1450)	0.1217 (0.1132 to 0.1319)
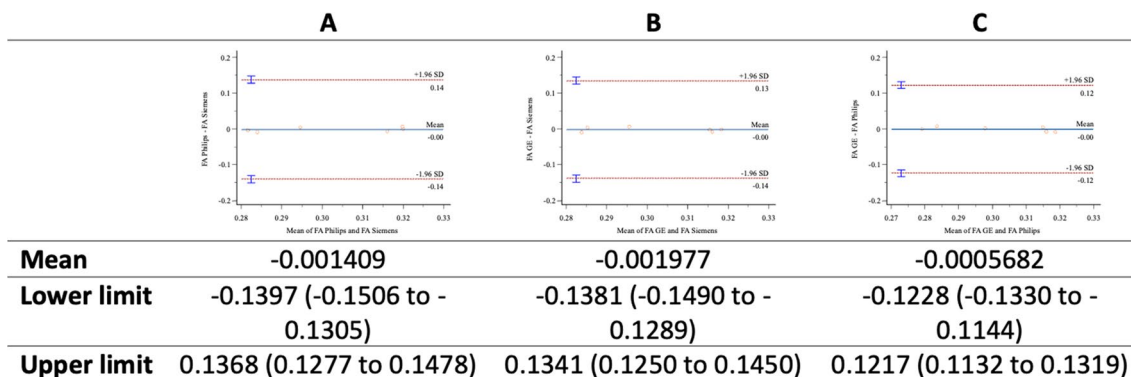
Fig. 4 FA-**A**: Philips versus Siemens; **B**: GE versus Siemens; **C**: GE versus Philips

Chianca *et al. Insights into Imaging* (2023) 14:32

Page 7 of 9

	A	B	C
Mean	-0.05080	-0.02858	0.02222
Lower limit	-0.8138 (-0.9753 to -0.7171)	-0.8589 (-1.0322 to -0.7558)	-0.5815 (-0.6470 to -0.5304)
Upper limit	0.7122 (0.6155 to 0.8737)	0.8018 (0.6987 to 0.9750)	0.6259 (0.5748 to 0.6914)
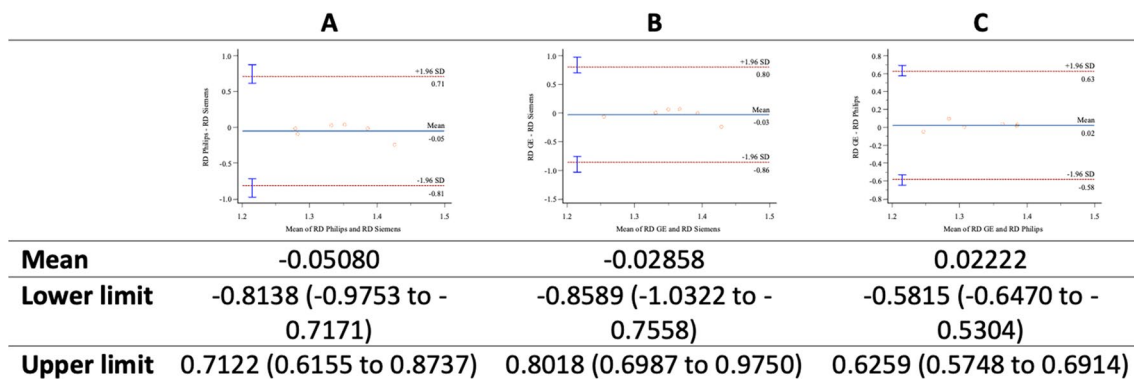
Fig. 5 RD-**A**: Philips versus Siemens; **B** GE versus Siemens; **C** GE versus Philips

of the muscular values as the results of the same effect described by Polders et al., who found a higher uncertainty in peripheral areas of the brain on 7 T [29].

Interestingly, one study conducted on 18 healthy subjects on a single 3 T MR (Philips Medical Systems, Best, Netherlands) on the entire lower leg [30] and reported a statistically significant intra-muscle difference in FA between the origin of the muscle and the muscle belly. This is probably due to different chemical–physical properties of the actin-myosin components and the different amount and organization of collagen fibres.

M-DTI may be influenced by contraction and activity. Muscle contraction induces muscle fibre shortening and increases cross-sectional area (CSA), producing higher MD and lower FA values. Mazzoli et al. [31] performed MRI examinations of the lower leg on five volunteers during muscle contraction and found lower FA values of anterior tibialis in dorsiflexion compared with plantar-flexion contraction and no contraction. The assessment of DTI values during muscle contraction is complex due to the length of current MRI sequences, which do not allow for constant, homogeneous fibre contraction. For this reason, we preferred to perform our MR examinations during muscle rest state. However, it is possible that in the future, with the increasingly widespread use of ultra-fast MRI sequences, the evaluation of muscle contraction will soon become available [32].

M-DTI may be influenced by activity, as well [33]. Hooijmans and colleagues described higher DTI values in upper legs muscles of 12 marathon runners in the post-marathon acquisition. The increase of MD and the decrease of FA are related to interstitial oedema and the alteration of diffusivity cellular barriers caused by muscle micro-trauma. These higher values returned to baseline (i.e. those values observed in the pre-marathon phase at the follow-up) after 3 weeks. MD and RD values are the first to return to the resting phase values, while FA values show a more prolonged alteration. This is the reason why we acquired MR examinations on the same days (within 6 h), without any sport activities performed the 4 weeks before the MR examination [34].

The first limitation of our study is the small sample size of volunteers, anyhow we assessed a large amount of data. Second, MR protocol parameters are not perfectly identical among the three MR scanners, because vendor-specific characteristics prevented us from applying exactly the same parameters for all the MR. However, other authors have used coils with different numbers of channels and DTI sequences with slightly different parameters to evaluate inter-observer and intra-observer agreement on the brain, obtaining promising results [13]. Moreover, the good results obtained with some parametric differences indirectly allow to obtain an even more significant inter-vendor agreement for clinical applications.

We believe that these reasons would make this sequence even more usable in clinical practice.

However, other studies with a larger sample of healthy volunteers are needed to confirm this claim.

Conclusions
Our results highlight the inter-vendor and inter-reader reproducibility of m-DTI values, and we strongly believe that the use of this sequence should be more included in the MRI protocols during daily clinical practice for the evaluation of MSK pathologies.

Abbreviations

CSA	Cross-sectional area
FA	Fractional anisotropy
ICC	Intra-class correlation coefficient.
IQR	Interquartile ranges
MD	Mean diffusivity
M-DTI	Muscle diffusion tensor imaging
MR	Magnetic resonance
MSK	Musculoskeletal
RD	Radial diffusivity
ROIs	Muscle regions of interest
T	Tesla

Chianca *et al. Insights into Imaging*   (2023) 14:32

Page 8 of 9

Supplementary Information

> **Additional file 1**: **Table S1**. DTI values of each single muscle ROI of the arms of both observers. **Table S2**. DTI values of each single muscle ROI of the legs of both observers. **Table S3**. DTI values of each single muscle ROI of the thighs of both observers.

Author contributions

VC helped in conceptualization, data curation, measurements, and writing— original draft. DA contributed to methodology and measurements. SR helped in software and formal analysis. LMS was involved in review and data curation. MM reviewed the manuscript. FDG performed supervision and methodology. All authors read and approved the final manuscript.

Funding

Availability of data and materials

The datasets used and/or analyzed during the current study are available from the corresponding author on reasonable request.

Declarations

Ethics approval and consent to participate

It was obtained from Swissethics, with waiver of informed consent.

Consent for publication

The authors of this manuscript received consent for publication.

Competing interests

LMS is a member of the Insights into Imaging Advisory Editorial Board. He has not taken part in the review or selection process of this article. All remaining authors declare that they have no conflict of interest.

Author details

[1]Clinica di Radiologia EOC IIMSI, Lugano, Switzerland. [2]Ospedale Evangelico Betania, Via Argine 604, 80147 Naples, Italy. [3]IRCCS Istituto Ortopedico Galeazzi, Milan, Italy. [4]Department of Radiology and Nuclear Medicine, Amsterdam University Medical Centres, University of Amsterdam, Amsterdam, The Netherlands. [5]Amsterdam Movement Sciences Research Institute, Amsterdam, The Netherlands. [6]Department of Biomedical Sciences for Health, University of Milano, Milan, Italy.

References

1. Chianca V, Albano D, Messina C et al (2017) Diffusion tensor imaging in the musculoskeletal and peripheral nerve systems: from experimental to clinical applications. Eur Radiol Exp 1:12
2. Zaraiskaya T, Kumbhare D, Noseworthy MD (2006) Diffusion tensor imaging in evaluation of human skeletal muscle injury. J Magn Reson Imaging 24:402–408
3. Bruno F, Arrigoni F, Mariani S et al (2019) Advanced magnetic resonance imaging (MRI) of soft tissue tumors: techniques and applications. Radiol Med 124:243–252
4. Chianca V, Albano D, Messina C et al (2021) An update in musculoskeletal tumors: from quantitative imaging to radiomics. Radiol Med 126:1095–1105. https://doi.org/10.1007/s11547-021-01368-2
5. Wheeler-Kingshott CAM, Cercignani M (2009) About "axial" and "radial" diffusivities. Magn Reson Med 61:1255–1260
6. HeeMSKerk AM, Sinha TK, Wilson KJ, Ding Z, Damon BM (2010) Repeatability of DTI-based skeletal muscle fiber tracking. NMR Biomed 23:294–303
7. Budzik J-F, Balbi V, Verclytte S, Pansini V, Le TV, Cotten A (2014) Diffusion tensor imaging in musculoskeletal disorders. Radiographics 34:E56–E72
8. Williams SE, HeeMSKerk AM, Welch EB, Li K, Damon BM, Park JH (2013) Quantitative effects of inclusion of fat on muscle diffusion tensor MRI measurements. J Magn Reson Imaging 38:1292–1297
9. Li GD, Liang YY, Xu P, Ling J, Chen YM (2016) Diffusion-tensor imaging of thigh muscles in Duchenne muscular dystrophy: correlation of apparent diffusion coefficient and fractional anisotropy values with fatty infiltration. AJR Am J Roentgenol 206:867–870
10. Van Dyck P, Froeling M, De Smet E et al (2017) Diffusion tensor imaging of the anterior cruciate ligament graft. J Magn Reson Imaging 46:1423–1432
11. Van Dyck P, Billiet T, Desbuquoit D et al (2020) Diffusion tensor imaging of the anterior cruciate ligament graft following reconstruction: a longitudinal study. Eur Radiol 30:6673–6684
12. Giraudo C, Motyka S, Weber M, Feiweier T, Trattnig S, Bogner W (2019) Diffusion tensor imaging of healthy skeletal muscles: a comparison between 7 T and 3 T. Invest Radiol 54:48–54
13. Min J, Park M, Choi JW, Jahng GH, Moon WJ (2018) Inter-vendor and inter-session reliability of diffusion tensor imaging: implications for multicenter clinical imaging studies. Korean J Radiol 19:777–782
14. Galbán CJ, Maderwald S, Uffmann K, Ladd ME (2005) A diffusion tensor imaging analysis of gender differences in water diffusivity within human skeletal muscle. NMR Biomed 18:489–498
15. Jovicich J, Marizzoni M, Bosch B et al (2014) Multisite longitudinal reliability of tract-based spatial statistics in diffusion tensor imaging of healthy elderly subjects. Neuroimage 101:390–403
16. Teipel SJ, Reuter S, Stieltjes B et al (2011) Multicenter stability of diffusion tensor imaging measures: a European clinical and physical phantom study. Psychiatry Res Neuroimaging 194:363–371
17. Vollmar C, O'Muircheartaigh J, Barker GJ et al (2010) Identical, but not the same: intra-site and inter-site reproducibility of fractional anisotropy measures on two 3.0T scanners. Neuroimage 51:1384–1394
18. Kermarrec E, Budzik JF, Khalil C, Le Thuc V, Hancart-Destee C, Cotten A (2010) In vivo diffusion tensor imaging and tractography of human thigh muscles in healthy subjects. AJR Am J Roentgenol 195:W352-366. https://doi.org/10.2214/AJR.09.3368
19. Damon BM (2008) Effects of image noise in muscle diffusion tensor (DT)-MRI assessed using numerical simulations. Magn Reson Med 60:934–944
20. Grech-Sollars M, Hales PW, Miyazaki K et al (2015) Multi-centre reproducibility of diffusion MRI parameters for clinical sequences in the brain. NMR Biomed 28:468–485
21. Magnotta VA, Matsui JT, Liu D et al (2012) MultiCenter reliability of diffusion tensor imaging. Brain Connect 2:345–355
22. Fox RJ, Sakaie K, Lee JC et al (2012) A validation study of multicenter diffusion tensor imaging: reliability of fractional anisotropy and diffusivity values. AJNR Am J Neuroradiol 33:695–700
23. Barp A, Carraro E, Albamonte E et al (2020) Muscle MRI in two SMA patients on nusinersen treatment: a two years follow-up. J Neurol Sci 417:117067
24. Ponrartana S, Ramos-Platt L, Wren TAL et al (2015) Effectiveness of diffusion tensor imaging in assessing disease severity in Duchenne muscular dystrophy: preliminary study. Pediatr Radiol 45:582–589
25. Otto LAM, van der Pol WL, Schlaffke L et al (2020) Quantitative MRI of skeletal muscle in a cross-sectional cohort of patients with spinal muscular atrophy types 2 and 3. NMR Biomed 33:e4357. https://doi.org/10.1002/nbm.4357
26. Fouré A, Ogier AC, Le Troter A et al (2018) Diffusion properties and 3D architecture of human lower leg muscles assessed with ultra-high-field-strength diffusion-tensor MR imaging and tractography: reproducibility and sensitivity to sex difference and intramuscular variability. Radiology 287:592–607
27. Yao X, Yu T, Liang B, Xia T, Huang Q, Zhuang S (2015) Effect of increasing diffusion gradient direction number on diffusion tensor imaging fiber tracking in the human Brain. Korean J Radiol 16:410–418
28. Froeling M, Nederveen AJ, Nicolay K, Strijkers GJ (2013) DTI of human skeletal muscle: the effects of diffusion encoding parameters, signal-to-noise ratio and T2 on tensor indices and fiber tracts. NMR Biomed 26:1339–1352
29. Polders DL, Leemans A, Hendrikse J, Donahue MJ, Luijten PR, Hoogduin JM (2011) Signal to noise ratio and uncertainty in diffusion tensor imaging at 1.5, 3.0, and 7.0 Tesla. J Magn Reson Imaging 33:1456–1463

30. Schlaffke L, Rehmann R, Froeling M et al (2017) Diffusion Tensor Imaging of the Human Calf: variation of Inter- and Intramuscle-Specific Diffusion. Parameters 46:1137–1148
31. Mazzoli V, Moulin K, Kogan F, Hargreaves BA, Gold GE (2021) Diffusion tensor imaging of skeletal muscle contraction using oscillating gradient spin Echo. Front Neurol 15(12):608549
32. Del Grande F, Rashidi A, Luna R et al (2021) Five-minute five-sequence knee MRI using combined simultaneous multislice and parallel imaging acceleration: comparison with 10-minute parallel imaging knee MRI. Radiology 299:635–646
33. Hooijmans MT, Monte JRC, Froeling M et al (2020) Quantitative MRI reveals microstructural changes in the upper leg muscles after running a marathon. J Magn Reson Imaging 52:407–417
34. Froeling M, Oudeman J, Strijkers GJ (2015) Muscle changes detected with diffusion-tensor imaging after long-distance running. Radiology 274:548–562. https://doi.org/10.1148/radiol.14140702

Publisher's Note